NCEP and GISS solar radiation data sets available for ecosystem modeling: Description, differences, and impacts on net primary production

Jeffrey A. Hicke
Natural Resource Ecology Laboratory, Colorado State University, Fort Collins, Colorado, USA

Received 20 October 2004; revised 21 January 2005; accepted 8 February 2005; published 15 April 2005.

[1] Downwelling surface solar radiation is an important input to ecosystem models, and global models require spatially extensive data sets that vary interannually to capture effects that potentially drive changes in ecosystem function. In this paper, I describe and compare solar radiation data sets from two representative sources, National Centers for Environmental Prediction (NCEP) reanalyses and Goddard Institute for Space Studies (GISS) calculations that included satellite observations of cloud properties. The CASA ecosystem model, which uses solar radiation and satellite-derived vegetation information, was run with the two solar radiation data sets to explore how differences affect estimated net primary production (NPP). GISS solar radiation matched ground-based observations better than NCEP solar radiation. Mean global NCEP solar radiation exceeded that from GISS by 16%, likely as a result of lower cloudiness within the NCEP reanalyses compared to satellite observations. Neither data set resulted in a significant trend over the study period (1984–2000). Locally, relative differences were up to 40% in the mean and 10% in the trend of solar radiation and NPP, and varied in sign across the globe. Because reanalysis solar radiation is only indirectly constrained by observations in contrast to the satellite-derived data, it is recommended that studies use the GISS solar radiation when possible.

Citation: Hicke, J. A. (2005), NCEP and GISS solar radiation data sets available for ecosystem modeling: Description, differences, and impacts on net primary production, *Global Biogeochem. Cycles*, *19*, GB2006, doi:10.1029/2004GB002391.

1. Introduction

[2] Models, input data sets, and computing power have advanced sufficiently such that in the last decade, estimates of ecosystem properties have become available at the global scale. Interest in the global carbon (C) cycle and its relationship to future climate change has led to studies of global C stocks and fluxes. Results have been used to quantify regional or global net carbon balance, identify locations with carbon sources or sinks, and propose mechanisms that drive these responses [*Cao et al.*, 2002; *Hicke et al.*, 2002a; *McGuire et al.*, 2001; *Nemani et al.*, 2002; *Nemani et al.*, 2003; *Potter et al.*, 1999; *Schimel et al.*, 2000].

[3] Solar radiation, used to prescribe photosynthetically active radiation (PAR) at the top of the canopy, is among the inputs required by ecosystem models. Although solar radiation inputs are sometimes limited to capturing the annual cycle due to the lack of data (e.g., historical runs such as reported by *McGuire et al.* [2001]), solar radiation does vary in time. Downwelling surface solar radiation has decreased by 1–3% per decade over the last 50 years as indicated by ground-based measurements (though the time periods varied among studies) [*Cohen et al.*, 2004; *Gilgen et al.*, 1998; *Liepert*, 2002; *Stanhill and Cohen*, 2001], consistent with decreases in pan evaporation over the last 50 years [*Roderick and Farquhar*, 2002]. Behavior in the 1990s suggests a recovery, however [*Cohen et al.*, 2004]. Responsible mechanisms include changing aerosol and cloud properties [*Liepert*, 2002; *Stanhill and Cohen*, 2001].

[4] Spatiotemporal variability in solar radiation can significantly affect carbon fluxes. In their study of global NPP trends, *Nemani et al.* [2003] reported large increases in NPP in the tropics driven by increasing solar radiation from NCEP. *Hicke et al.* [2002b] compared conterminous United States NPP calculated using National Centers for Environmental Prediction (NCEP) solar radiation with that computed with data from the VEMAP project [*VEMAP Members*, 1995]. NPP trends over 12 years were similar with the two sets of input data, but the higher NCEP solar radiation resulted in higher NPP by ~10%.

[5] For model inputs of temperature and precipitation, multiple sources of data exist that satisfy the necessary requirements of global extent and interannual variability (e.g., from NCEP reanalyses [*Kistler et al.*, 2001]). In contrast, solar radiation is not recorded operationally by weather stations, and coverage of ground-based instruments

0886-6236/05/2004GB002391$12.00

is sparse. Global estimates of solar radiation therefore rely on models of the propagation of radiation through the atmosphere together with information about atmospheric conditions that affect this propagation. The physical processes governing radiative transfer through the atmosphere are well known, and with adequate knowledge of the state of the atmosphere, the solar radiation incident at the surface can be calculated with sufficient accuracy for use in ecosystem models. Even highly parameterized, fast radiative transfer models suitable for inclusion into general circulation models (GCMs) calculate incident solar radiation to within 4–11% (compared to results from more detailed models) [*Fouquart et al.*, 1991].

[6] Several types of global solar radiation data sets exist. The first type is produced with a GCM that assimilates observations of the atmosphere. In addition to producing global, physically consistent estimates of temperature, pressure, and winds that are constrained by observations, the GCM uses representations of other important processes such as clouds, radiation, and the land surface to model a suite of atmospheric and surface variables.

[7] A second type of solar radiation data set is calculated using a radiative transfer model (similar to ones used in reanalysis projects) together with satellite-derived atmospheric properties, most importantly clouds. Global satellite observations of cloud variables have become available as part of the International Satellite Cloud Climatology Project (ISCCP). Several groups have used the ISCCP cloud variables together with other information about the atmosphere (e.g., water vapor, aerosols) to compute radiation fluxes [*Darnell et al.*, 1992; *Pinker and Laszlo*, 1992; *Zhang et al.*, 1995, 2004]. While limited to the time period of ISCCP data availability and thus satellite observations, the use of direct observations of clouds in these data sets provides a comparison of radiative fluxes to those from reanalyses.

[8] A third type of data set estimates solar radiation from other climate variables. An example is the CLIMSIM model, which uses temperature and precipitation to estimate incident solar radiation [*Running et al.*, 1987].

[9] The goals of this study were to describe two representative solar radiation data sets available for input to global ecosystem models, to quantify differences in the two data sets, and to explore how possible differences affect estimates of NPP using the CASA ecosystem model [*Potter et al.*, 1993]. The NCEP reanalysis was utilized owing to its spatial and temporal extent, online availability, and inclusion in recent studies. The Goddard Institute for Space Studies (GISS) satellite-derived data set was produced by the same team that developed the ISCCP data set, is the longest time series of solar radiation estimates of the several ISCCP-based data sets available, and incorporated the latest version of ISCCP cloud information. I compared the GISS and NCEP solar radiation against observations from a ground-based data set, and investigated differences in the mean spatial patterns of these two global data sets as well as in the temporal trends. Effects on spatiotemporal patterns of NPP are presented. Absolute differences between the two data sets are discussed in addition to relative differences to allow for comparisons of magnitudes among regions. The study will inform future ecosystem modeling studies that include solar radiation as an input.

2. Data Sets and Models

2.1. Solar Radiation

2.1.1. NCEP

[10] The NCEP reanalysis (www.emc.ncep.noaa.gov/research/mrf.html) [*Phillips*, 1996] is based on the National Meteorological Center (NMC) model described by *Kanamitsu* [1989]. The calculation of shortwave radiation uses the method of *Lacis and Hansen* [1974] to account for multiple scattering by the adding/doubling method as well as for gaseous absorption by O_3 and water vapor (Table 1). CO_2 absorption follows that described by *Sasamori et al.* [1972]. O_3 and CO_2 are prescribed using climatologies; water vapor is predicted by the NMC model; and clouds are diagnosed from model-predicted relative humidity, vertical motion, and convective rain similar to *Slingo* [1987]. Cloud radiative properties (e.g., optical depth) are specified as a function of cloud pressure thickness and temperature following *Harshvardhan et al.* [1989].

[11] Updates to the NMC model that affected solar radiation calculations included changes to the convection parameterization scheme and diagnostic cloud scheme [*Kalnay et al.*, 1996]. These changes improved precipitation and outgoing longwave radiation estimates compared to observations.

[12] The NCEP reanalysis surface radiation is available every 6 hours from 1948 to the present. For this study, I averaged the mean daily radiation, available online from the NOAA Climate Diagnostics Center (www.cdc.noaa.gov), over each month during the time period of interest (1984–2000).

[13] Reanalysis output variables were subjectively classified by *Kalnay et al.* [1996] according to how strongly each variable was influenced by observations. Downwelling surface solar radiation is considered a category C variable, which indicates that no observations directly affect this variable. The authors advised caution in interpreting the results of class C variables.

[14] Multiple studies have evaluated the NCEP surface radiation. *Bony et al.* [1997] compared 2 years of data over the tropical oceans to satellite-derived radiation calculated by *Darnell et al.* [1992] and *Pinker and Laszlo* [1992], and found that the NCEP reanalyses systematically underestimate the net solar radiation by 10–30 W m^{-2}. Despite this, Bony et al. reported that the NCEP total cloud fraction was less than the ISCCP cloud fraction by 10–20%, and so suggested that differences occurred owing to differences in cloud radiative properties. Similar conclusions for additional years, for land as well as ocean, and for latitudes equatorward of 60° were reached by *Weare* [1997]. With 4 years of ocean radiative fluxes, *Scott and Alexander* [1999] found spatial variability in differences between NCEP and satellite-derived net surface shortwave fluxes, depending on cloud type. Furthermore, NCEP interannual variability exceeded the satellite-derived variability in some regions, while the reverse was true in other regions. *Ladd and Bond* [2002] found that NCEP reanalyses overestimated

Table 1. Comparison of Solar Radiation Data Sets

Data Set	Temporal Extent and Resolution	Radiative Transfer Model	Cloud Macroscopic Properties (Cover Fraction, Top Pressure, and Temperature)	Cloud Radiative Properties (Optical Depth, Effective Radius)	Inclusion of Aerosols (Source)?	Other Inputs
NCEP reanalysis	1948 to present; every 6 hours	*Lacis and Hansen* [1974] adding/doubling for O_3, water vapor; *Sasamori et al.* [1972] CO_2 absorption	model-derived	f(cloud top pressure, temperature, thickness) following *Harshvardhan et al.* [1989]	no	T, water vapor: model-derived
GISS	July 1983 to June 2001; every 3 hours	GISS GCM [*Hansen et al.*, 2002]; uses adding/doubling method and correlated k-distribution method (a generalization of and improvement to *Lacis and Hansen* [1974])	ISCCP D retrievals; includes phase (liquid versus ice)	ISCCP D retrievals	yes; interannually varying stratospheric aerosols from SAGE II satellite observations	T, water vapor (TOVS); O_3 (TOMS)

downwelling surface solar radiation by 70–80 W m^{-2} in the Bering Sea and by 20 W m^{-2} in the northeast Pacific Ocean compared to mooring data, likely resulting from inaccurate representation of clouds in the model. *Yang et al.* [1999] reported that global NCEP reflected solar radiation was overestimated compared to ERBE data. They found good agreement with clear-sky fluxes, however, implying deficiencies in the NCEP cloud parameterizations that are currently being investigated.

2.1.2. GISS

[15] The International Satellite Cloud Climatology Project (ISCCP) combines observations from geostationary and polar-orbiting satellites to retrieve global cloud properties at diurnal, seasonal, and interannual scales. Cloud variables retrieved include cover fraction, top pressure and temperature, and optical depth. Data collection began in July 1983, and cloud information is available at different spatial resolutions, including 30-km data from individual satellites as well as a gridded product (280 km). The latest version ("D") includes numerous updates, including revised calibrations and improved cloud detection over land [*Rossow and Schiffer*, 1999]. Currently, cloud information is available from July 1983 through June 2001, but additional data will become available at least through 2006 [*Zhang et al.*, 2004]. The GISS solar radiation calculation used these cloud properties to calculate radiative fluxes.

[16] The radiative transfer model employed to compute the GISS data set was a new version of the GISS GCM [*Hansen et al.*, 2002] (Table 1). The original version is described by *Hansen et al.* [1983]. Significant updates to the radiative transfer model relevant to downwelling surface shortwave fluxes include additional spectral resolution, the incorporation of temporally varying aerosols, and improved cloud parameterizations such as the better representation of ice clouds [*Zhang et al.*, 2004]. The GISS GCM model considers gaseous absorption (all radiatively significant gases) in a multiple scattering, vertically inhomogeneous atmosphere from the surface to the top of the atmosphere (TOA). The adding/doubling method of *Lacis and Hansen* [1974] to account for multiple scattering when computing fluxes is the same as employed in the NCEP model. However, the GISS model uses the correlated k-distribution to represent the spectral dependence of radiative fluxes, which is a generalization of the method described by *Lacis and Hansen* [1974] and is more accurate for inhomogeneous atmospheres (such as Earth's) [*Hansen et al.*, 1983]. Fifteen non-contiguous spectral intervals are used to compute the shortwave fluxes. Radiative fluxes are computed globally every 3 hours at 280-km spatial resolution.

[17] The GISS radiative transfer model was modified to accommodate atmospheric inputs that replace those provided by the GCM [*Zhang et al.*, 1995, 2004]. Temperature and water vapor profiles were specified from the TIROS Operational Vertical Sounder (TOVS) data set produced by NOAA [*Kidwell*, 1995]. Ozone was taken from the Total Ozone Mapping Spectrometer (TOMS) [*McPeters et al.*, 1996]. Tropospheric climatological and interannually varying stratospheric aerosols were included; stratospheric aerosols were specified by Stratospheric Aerosol and Gas Experiment II (SAGE II) satellite observations [*Sato et al.*, 1993].

[18] Clouds were defined in the model by the ISCCP cloud top temperature and climatological cloud pressure increment. Cloud cover fraction, optical depth, and water path were also taken from the ISCCP data set. Radiative fluxes from this new version as well as an earlier version of this data set that used a previous release of ISCCP cloud variables ("C" instead of "D") were compared to various other radiative flux estimates [*Rossow and Zhang*, 1995; *Zhang et al.*, 2004], including (1) TOA fluxes as measured by the Earth Radiation Budget Experiment (a series of satellites that were in operation during the late 1980s) as well as fluxes observed by the CERES satellite instrument, (2) the Global Energy Balance Archive [*Ohmura and Gilgen*, 1991] and the Baseline Surface Radiation Network [*Ohmura et al.*, 1998] data sets consisting of ground-based flux measurements supplemented by satellite analyses and bulk transfer formulas, and (3) additional local

ground-based measurements. Resulting uncertainties were estimated to be 5–10 W m^{-2} at the top of the atmosphere and 10–15 W m^{-2} at the surface for regional and monthly means [*Zhang et al.*, 2004]. Specifically, comparison of downwelling surface solar radiation with the Baseline Surface Radiation Network data [*Ohmura et al.*, 1998] revealed a mean difference of 2 W m^{-2}, a root-mean squared error of 19 W m^{-2}, and $r = 0.98$.

2.1.3. Growing Season Solar Radiation

[19] Because plant growth is close to zero in winter for most extratropical regions owing to temperature and light limitations, analysis of total annual radiation would include months when radiation is not important for computing NPP. Therefore total growing season solar radiation (GSS; J m^{-2} yr^{-1}) was computed for comparison between the two data sets,

$$\mathrm{GSS} = \sum S_{i,j}, \tag{1}$$

where $S_{i,j}$ was the solar radiation (W m^{-2}) during growing season month i at grid cell j. The growing season was defined as months when mean monthly NPP > 10% of the maximum mean monthly NPP for that grid cell. I report global solar radiation for land areas (S; J yr^{-1}) as the area-weighted sum of GSS across all land areas,

$$S = \sum \mathrm{GSS}_j \; A_j, \tag{2}$$

where A_j is the area of grid cell j.

2.1.4. GEBA Ground-Based Observations of Solar Radiation

[20] The Global Energy Balance Archive (GEBA) database stores information about observations of global solar radiation that have been collected at sites across the globe from 1922 to 1990 [*Gilgen and Ohmura*, 1999]. Quality control procedures have been applied to the data that allow for the screening of observations that may be in error. Global shortwave irradiances from 1405 stations were selected for comparison with the NCEP and GISS data; only those observations that were not flagged as erroneous were utilized. Mean GEBA solar radiation was computed for the NCEP and GISS grids from GEBA stations that fell within each grid cell. As a result of the sparseness of the GEBA database, most grid cells with any ground-based observations (about 150–200 per year) contained only one station, though in more densely populated regions, such as Europe, grid cells contained up to four stations. Comparisons between annual mean solar radiation data sets are shown, though using monthly data resulted in similar behavior.

2.2. Ecosystem Model

[21] The Carnegie-Ames-Stanford Approach (CASA) ecosystem model is a production-efficiency model driven by satellite data as well as temperature, precipitation, solar radiation, and land cover and soil classifications [*Field et al.*, 1995; *Potter et al.*, 1993]. CASA computes NPP as a function of the absorbed photosynthetically active radiation (APAR), a maximum potential light-use efficiency variable ε^*, and temperature (T_ε) and moisture (W_ε) scalars that represent climate stresses on vegetation light-use efficiency,

$$\mathrm{NPP} = \mathrm{fAPAR} \times \mathrm{PAR} \times \varepsilon^* \times T_\varepsilon \times W_\varepsilon, \tag{3}$$

where fAPAR is the fraction of APAR, solar radiation is converted to PAR by multiplying by 0.5, and fAPAR × PAR = APAR. Following *Los et al.* [2000], fAPAR is computed by using the linear relationships between fAPAR and the Normalized Difference Vegetation Index (NDVI) and fAPAR and the simple ratio (SR),

$$\mathrm{NDVI} = (\mathrm{NIR} - \mathrm{VIS})/(\mathrm{NIR} + \mathrm{VIS}), \tag{4}$$

$$\mathrm{SR} = \mathrm{NIR}/\mathrm{VIS}, \tag{5}$$

where NIR is the reflectance in the near infrared channel and VIS is the reflectance in the visible channel of the Advanced Very High Resolution Radiometer (AVHRR). *Los et al.* [2000] found that an average of fAPAR using NDVI and SR compared best with field observations.

[22] The Global Monitoring and Mapping Studies (GIMMS) NDVI processing algorithm [*Brown et al.*, 2005; *Los et al.*, 2000; *Tucker et al.*, 2001] corrects the index for influences that contaminate the data, such as differences in solar zenith angle, sensor degradation, intercalibration, and missing values. I used the GIMMS Version G of NDVI, released in July 2004, from 1984–2000, matching the availability of the GISS solar radiation data. I aggregated the monthly 8-km NDVI data to a spatial resolution of 0.5° by averaging the 50% of the 8-km cells with the highest NDVI. This method was a compromise between an average of all 8-km cells and the maximum NDVI in each 0.5° grid cell, and reduced cloud contamination in persistently cloudy regions while allowing for some spatial variability within each grid cell. The two solar radiation data sets, at 2.5° (GISS) and roughly 2° (NCEP) spatial resolution, were interpolated to the 0.5° NDVI grid cells.

[23] The maximum potential light-use efficiency ε^* (equation (3)) is set by a calibration step where CASA NPP is fit to field observations of NPP [*Potter et al.*, 1993]. In this study, I set ε^* to 0.46 for the runs using NCEP solar radiation, and to 0.50 for the runs using GISS solar radiation. The temperature and moisture scalars (T_ε and W_ε) are used to reduce ε^* in response to climate conditions that act to stress plants beyond what may be resolved in the NDVI [*Field et al.*, 1995]. T_ε and W_ε are computed at every location at each time step using climate data. Temperatures and precipitation were taken from Version TS 2.0 of the data set produced by the Climate Research Unit (CRU) (T. D. Mitchell et al., A comprehensive set of high- resolution grids of monthly climate for Europe and the globe: The observed record (1901–2000) and 16 scenarios (2001–2100), submitted to *Journal of Climate*, 2005). These data are interannually varying with 0.5° spatial resolution.

[24] The Moderate Resolution Imaging Spectroradiometer (MODIS) land cover product was aggregated from 1-km spatial resolution to 0.5° using the most common land cover class for each grid cell. The Food and Agriculture Organi-

zation (FAO)/UNESCO soil map specified soil texture in CASA [*FAO/UNESCO*, 1971].

3. Results

3.1. Comparison of Solar Radiation Data Sets

3.1.1. Evaluation With GEBA Ground-Based Observations

[25] Comparisons of annual means from the GISS and NCEP data sets with GEBA ground- based solar radiation revealed a reduced error in the GISS data set (Figure 1). Linear least squares fits to the data show that the GISS solar radiation more closely matched the GEBA data than the NCEP solar radiation in terms of slope (1.01 versus 0.87 for the NCEP fit), offset (4.9 versus 67.1), and R^2 (0.90 versus 0.87). The mean bias error (GISS or NCEP minus GEBA) and root-mean square error were substantially reduced in the GISS comparison (−6.45 versus −46.55 and 15.91 versus 49.18, respectively).

[26] Differences between mean annual solar radiation values were mapped to indicate areas covered by the GEBA database and to assess potential regional biases (Figure 2). GEBA coverage in Europe was excellent, and sparse but extensive throughout much of Asia, North America, and sub-Saharan Africa. Gaps in coverage exist, most notably for much of South America.

[27] NCEP radiation tended to be higher than GEBA values in Europe, eastern North America, and Africa. NCEP values exceeded GEBA values slightly in Asia and parts of North America, and substantially in Australia. Differences with GISS solar radiation exhibited similar patterns, though reduced in magnitude, except in coastal South America where differences were higher than those from the NCEP comparison.

3.1.2. Comparisons Between NCEP and GISS

[28] Global growing season radiation over land (S) averaged over the 17-year period was 69×10^{22} J yr^{-1} for the GISS data set, and 80×10^{22} J yr^{-1} for the NCEP data set, corresponding to a 16% difference (Figure 3). Interannual variability of S compared to the mean was low in both cases; coefficients of variability for both data sets were less than 1%. Despite this low global value, large regional variability occurred in the GISS GSS (4–6%; data not shown). Both data sets exhibited little temporal trend in S (<1% change over 17 years).

[29] Mean GSS declined from the tropics toward the poles (Figures 4a and 4b). Subtropical and tropical regions with little cloud cover, particularly those desert regions associated with the descending branch of the Hadley circulation, exhibited the highest values. Persistent cloud cover in the wet tropics reduced solar radiation there.

[30] NCEP GSS generally exceeded GISS GSS except in the Amazon River basin and in central Africa. The largest absolute differences occurred in South America, Africa, and Asia (Figure 4c). Relative differences between the data sets enhanced the higher latitudes, and ranged from >40% in many regions (NCEP higher) to 10% in the Amazon River basin (GISS higher).

[31] Trends in GSS over the 1984–2000 study period varied regionally despite little change in the global total

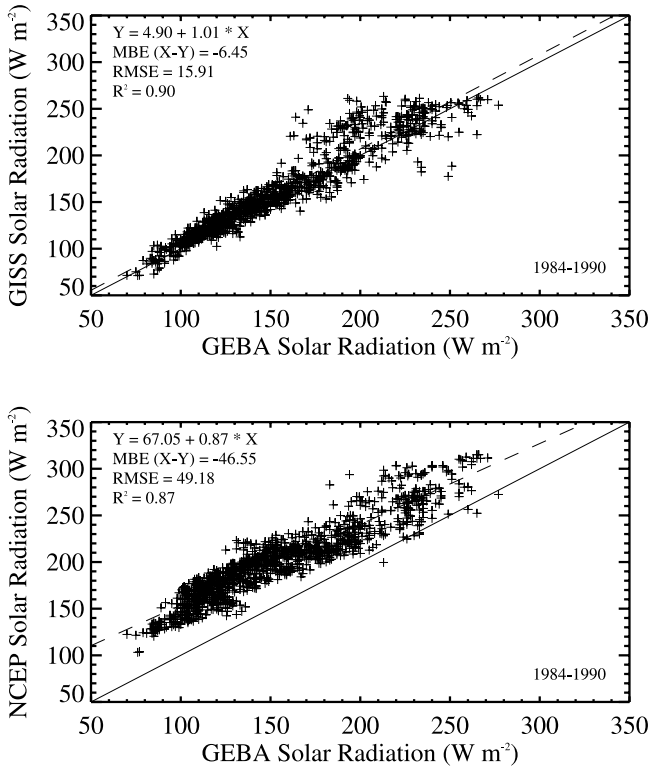

Figure 1. Comparison of ground-based GEBA solar radiation (W m^{-2}) with (top) GISS and (bottom) NCEP values. GEBA observations from different stations were averaged within NCEP and GISS grid cells. Each point represents 1 year and one grid cell. All available data are presented for the period 1984–2000; data are evenly distributed between 1984 and 1989, with 1990 having only a few values.

(Figure 5). Absolute increases were highest in southern North America, central South America, and parts of Africa and southern Asia (NCEP). Large decreases in the GISS data occurred in western North America, Africa, southern Asia, and Australia; NCEP GSS declined most in tropical South America and southern Africa. In many regions, changes corresponded to less than 5% over the 17-year period, though eastern Europe experienced a 10% increase and parts of northern North America and Asia had decreases of 10% in the GISS data.

[32] NCEP GSS trends were both higher and lower than GISS GSS trends, depending on region (Figure 6). The largest differences occurred in the tropics and subtropics, with the magnitude of NCEP changes greater than those from GISS (10% changes in the NCEP solar radiation, whereas 5% changes in the GISS data). Growing season solar radiation increased in both data sets in the Amazon River basin, though GISS had about a 5% change versus the 10% change in the NCEP data set.

3.2. Comparison of Resulting NPP

[33] The higher NCEP solar radiation resulted in slightly greater global NPP estimates (48.8 Pg C yr^{-1}) compared

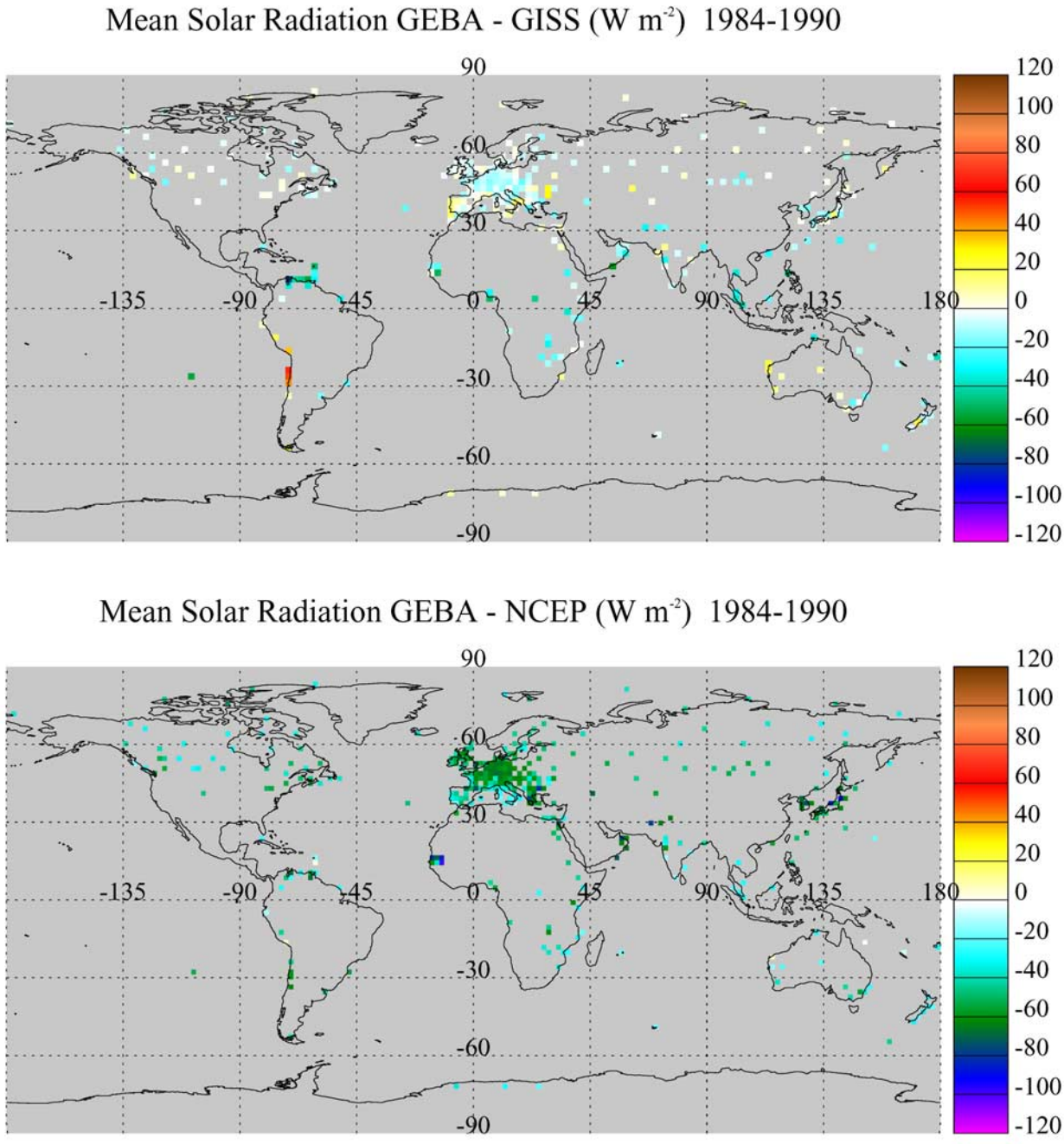

Figure 2. Differences in mean annual solar radiation (W m^{-2}) between GEBA and (top) GISS and (bottom) NCEP values.

to results using GISS solar radiation (47.7 Pg C yr^{-1}) (Figure 7). Both of these estimates were within the range of global NPP computed using different models and methods as reported by *Cramer et al.* [1999] (44–66 Pg C yr^{-1}). Only minor increases in global NPP (1.1% using NCEP radiation, 0.3% using GISS radiation) were computed over the 17-year study period using the two solar radiation data sets. Somewhat greater temporal variability occurred in the GISS NPP results compared to the NCEP NPP, as expected from the variability differences in the two estimates of *S*. However, the magnitude of the difference in NPP variability is less than differences in solar radiation variability. This indicates that the estimated NPP responded strongly to fAPAR, which is modified by many mechanisms (e.g., temperature, precipitation, land use) in addition to solar radiation.

[34] The minor difference in global NPP total between the runs with NCEP solar radiation and those with GISS solar radiation resulted from different values of ε^*. The ground-based studies used in the calibration of ε^* are limited in

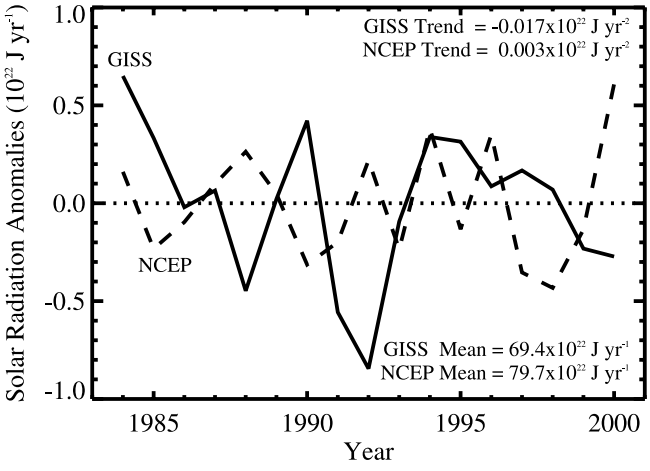

Figure 3. Global growing season solar radiation anomalies (10^{22} J yr^{-1}) from GISS (solid line) and NCEP (dashed line) data sets. GISS mean solar radiation is 16% less than NCEP.

spatial extent, resulting in the minor difference in global NPP totals. If ε^* were the same for both runs, differences in mean NPP would be greater.

[35] Mean NPP patterns (Figure 8) resulted from not only the input solar radiation but also from fAPAR as derived from satellite observations as well as from climate down-regulators that limit growth in suboptimal conditions. Thus, although NPP patterns decline from equator to pole following solar radiation, additional structure appears in the mean NPP map. Tropical forests had the highest NPP, while desert NPP was near zero, somewhat of a reversal of solar radiation patterns.

[36] Differences in mean NPP between the two runs varied substantially for different regions despite similar global values. In the extratropics, NPP from NCEP solar radiation exceeded that from GISS solar radiation by 50 g C m^{-2} yr^{-1}, corresponding to differences of 5–30% (Figure 8). In contrast, in the Amazon River basin, central Africa, and southeast Asia, NPP from GISS solar radiation was greater by 100 g C m^{-2} yr^{-1} or more (5–20%). Relative differences in mean NPP were similar to relative differences in mean solar radiation (see equation (3), though ε^* varies between the two runs). However, the large absolute differences in these tropical areas compared to other areas, in spite of small relative differences, underscores the importance of analyzing absolute and relative amounts.

[37] Similar to mean NPP, large changes in NPP from GISS solar radiation are evident regionally in spite of little change in global NPP (Figure 9). Particularly notable are increases in the north central United States, Brazil, parts of Eurasia, and the Sahel, and large decreases in eastern Mexico and throughout much of the tropics. Viewing the trends as percent increases enhances the response of dry and tundra areas, which generally increased; changes in tropical NPP ranged from a 10% reduction to a 20% increase.

[38] Absolute trend differences between NPP computed with GISS and with NCEP solar radiation were largest in the tropics, particularly in South America and Africa where both positive and negative differences occurred (Figure 10a). In terms of percent increases over the study period, NPP changes differed by 10% in these regions. Similar magnitude percent increase differences can be seen in Eurasia (Figure 10b).

3.3. Impacts of Solar Radiation on NPP Trends

[39] In this section, I discuss how changing solar radiation affects estimated NPP. Shifts in solar radiation can be manifested in the modeled NPP in two ways. The first is directly through the specification of PAR in equation (3). The second is indirectly through a change in vegetation in response to changing radiation conditions. This vegetation change would be revealed as a change in NDVI and therefore fAPAR. I explore these effects by analyzing time series of NPP inputs at one location and by investigating the effect of using a mean annual cycle of solar radiation in an additional global NPP run.

[40] I selected a location in British Columbia, Canada (see Figure 5b) that had the largest percent decrease in GISS solar radiation over the study period. Monthly trends in input variables and in the resulting NPP were computed and plotted relative to mean annual cycles (Figure 11). Solar radiation at this location decreased throughout the growing season, with the largest reductions occurring in the middle of summer. In contrast, fAPAR was nearly constant through much of the growing season, except in July, when it increased. NPP decreased slightly in the early growing season, then increased in July as a result of the fAPAR increase. Inspection of the precipitation trends reveals that precipitation increased substantially in July, likely causing the increase in fAPAR and NPP and counteracting the effects of reduced solar radiation. In fact, the decrease in solar radiation was probably linked to the increase in precipitation through enhanced cloudiness.

[41] To explore the direct effect of solar radiation, I calculated the mean annual cycle of GISS solar radiation at each grid cell, then used that to estimate NPP instead of using the interannually varying data set. NPP trend differences were largest in the Amazon River basin, where the use of interannually varying solar radiation increased trends by 4 g C m^{-2} yr^{-1} (Figure 12a). Weak enhancement of trends is evident in eastern Europe. Decreases occurred throughout much of the globe. Differences in relative increases were of the order of 5–10% in many locations (Figure 12b).

4. Discussion

[42] GISS solar radiation matched ground-based observations much better than NCEP values, a result consistent with other findings. Both the NCEP and GISS solar radiation data sets were computed with efficient radiative transfer models that were designed for use in GCMs. These models include parameterizations of radiative transfer processes to allow rapid estimation of radiative fluxes at high spatial and temporal frequency. Important radiative processes such as multiple scattering by molecules and cloud particles as well as absorption by the major gases and cloud particles are included in both models. Because (1) the physical processes

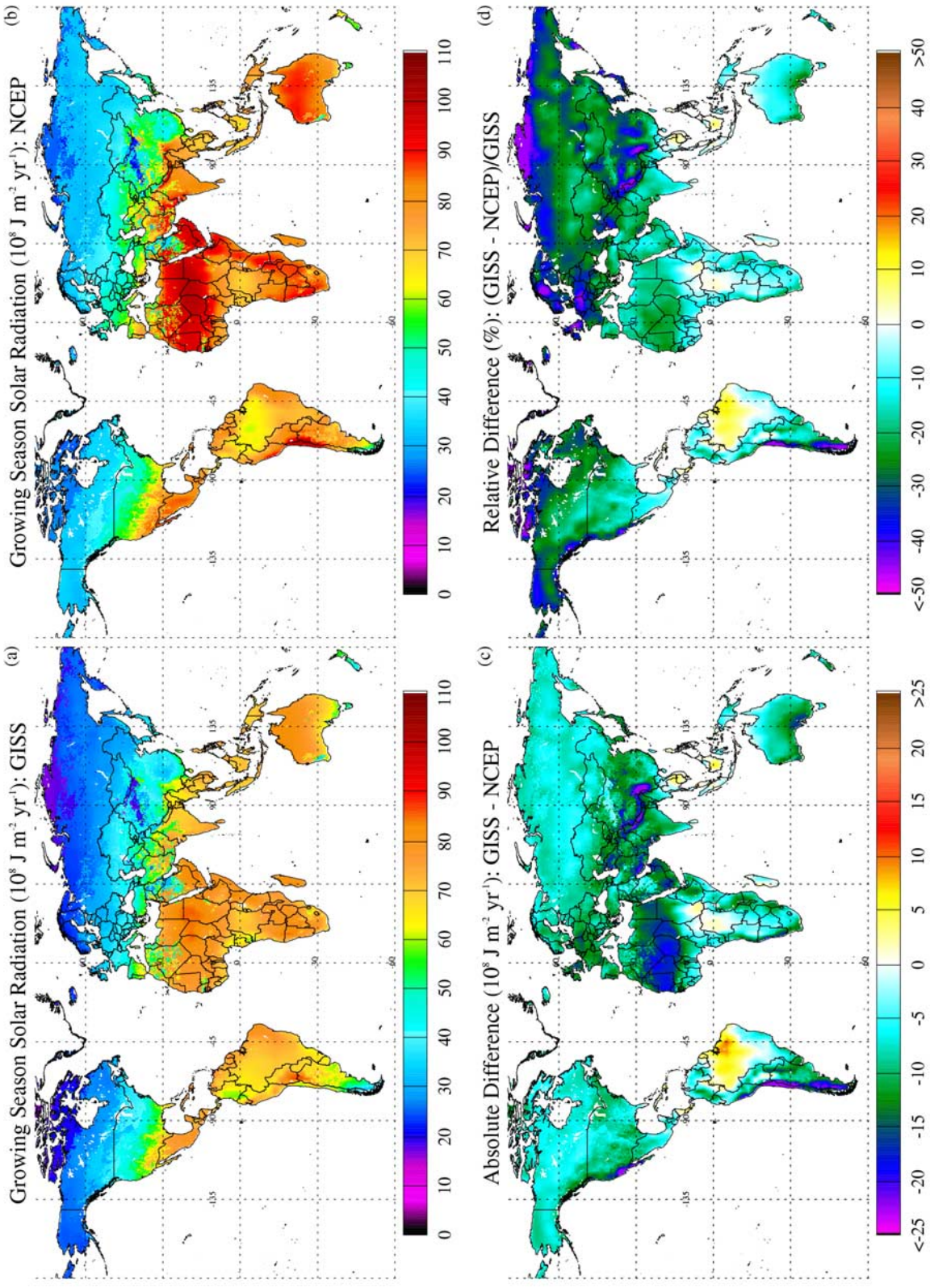

Figure 4. Growing season solar radiation averaged over 1984–2000 (10^8 J m^{-2} yr^{-1}) from (a) GISS and (b) NCEP data sets. (c) Absolute difference between GISS and NCEP (10^8 J m^{-2} yr^{-1}). (d) Relative difference (%).

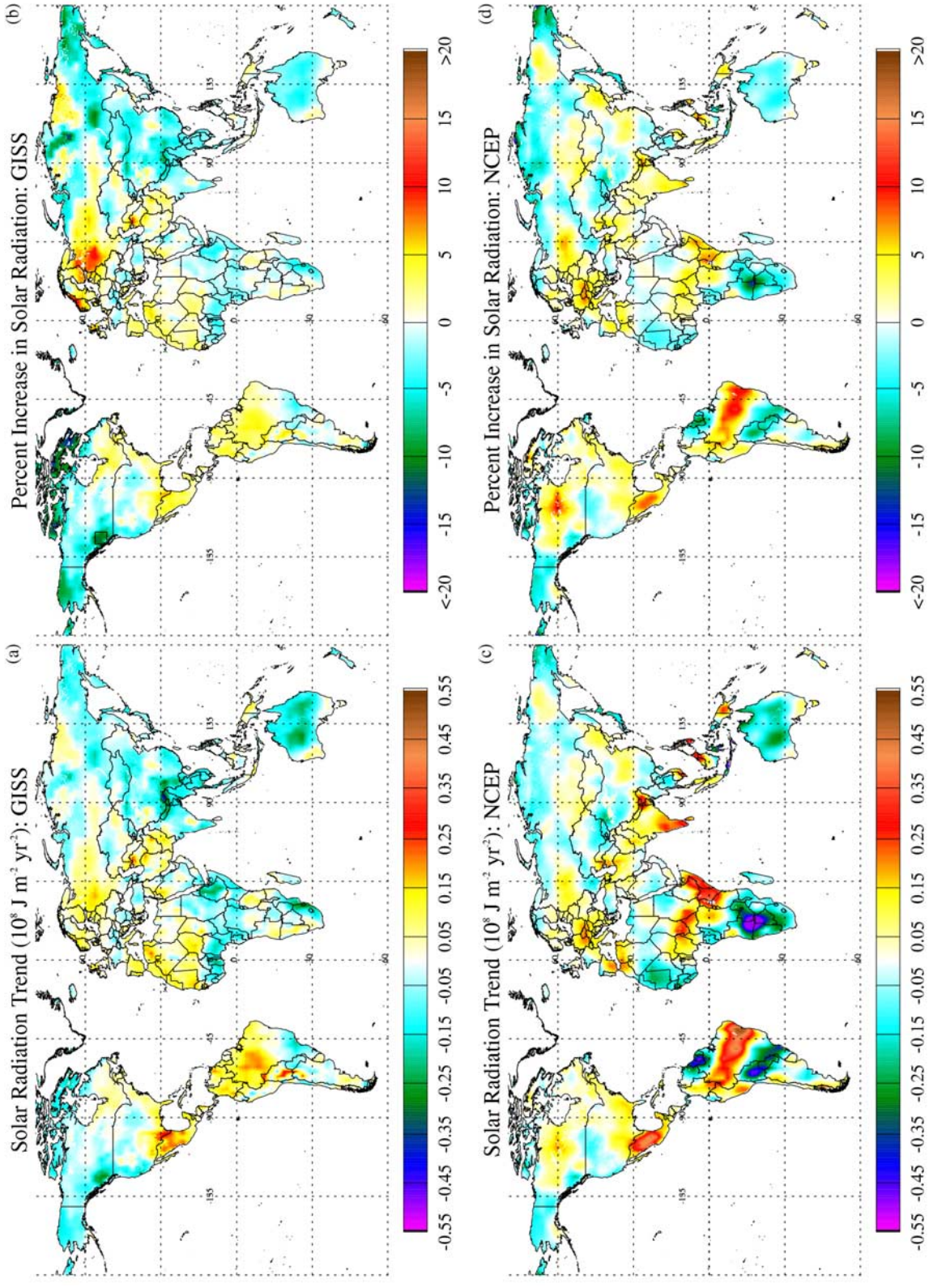

Figure 5. Trend in growing season solar radiation from 1984–2000. (a) Absolute trend from GISS data set (10^8 J m^{-2} yr^{-1}). (b) Percent increase from GISS. Square in British Columbia, Canada, shows location plotted in Figure 11. (c) Absolute trend from NCEP data set (10^8 J m^{-2} yr^{-1}). (d) Percent increase from NCEP.

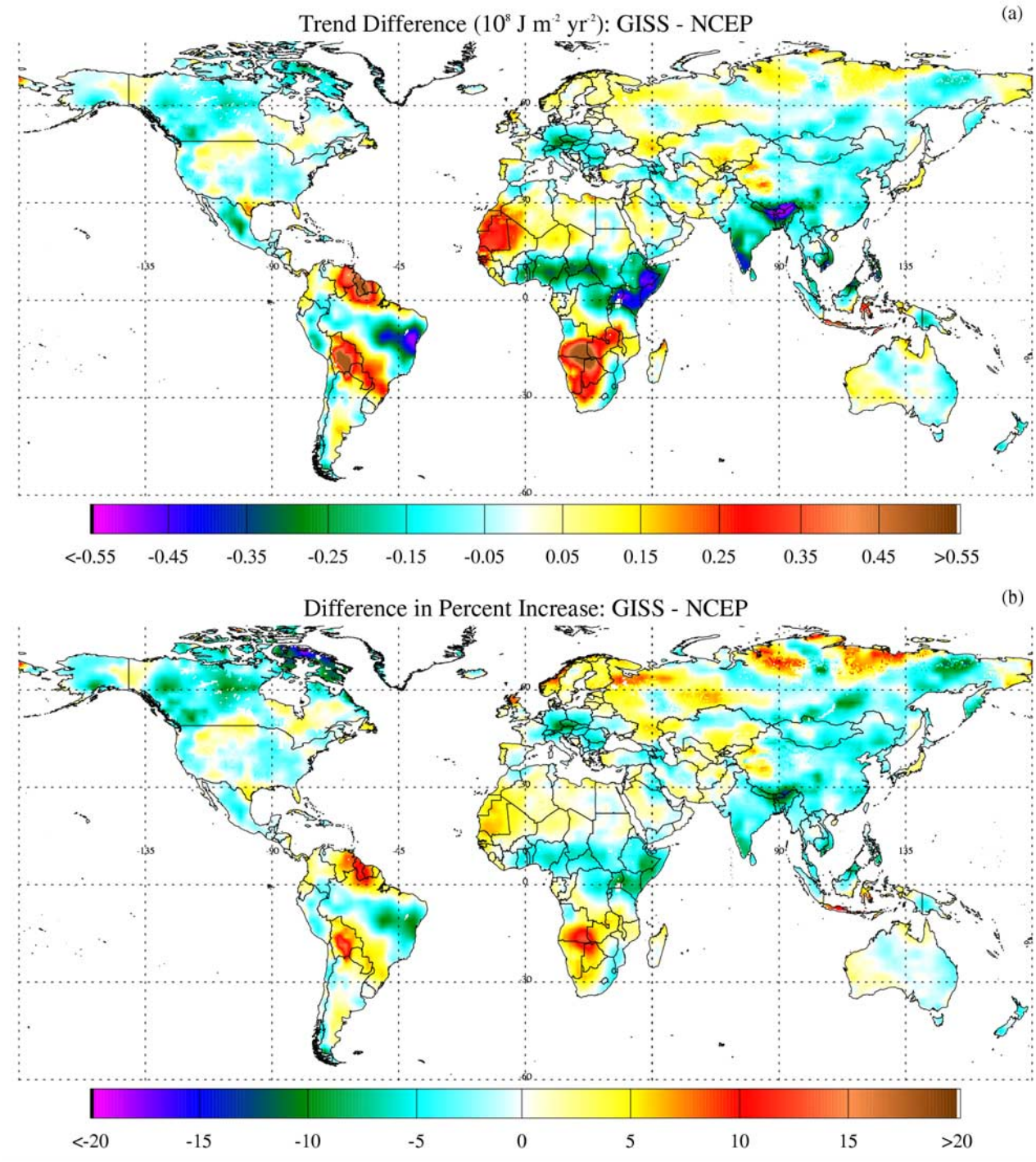

Figure 6. (a) Difference between GISS and NCEP absolute growing season solar radiation trends from 1984–2000 (10^8 J m^{-2} yr^{-1}). (b) Difference in percent increases.

involving radiative transfer are well known and well studied, (2) the parameterizations used are sufficiently accurate for surface solar fluxes [*Fouquart et al.*, 1991], and (3) the two models are similar in complexity (except that the GISS model accounts for aerosols), it is likely that differences in the solar radiation data sets are not attributable to differences in the radiative transfer modeling. Instead, the major differences are due to inputs, primarily clouds but also aerosols. Satellite observations of clouds (ISCCP) provide more confidence in the resulting GISS solar radiation data set than the model-derived clouds of NCEP. In addition, the inclusion of aerosol effects in the GISS data set, including interannually varying stratospheric aerosols, resulted in more realistic estimates.

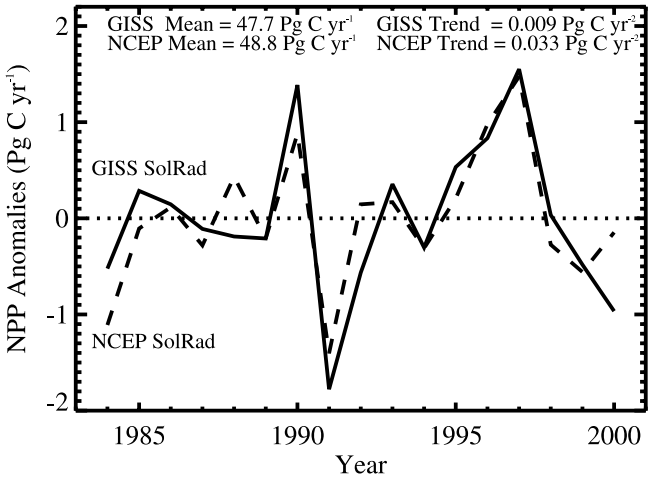

Figure 7. Global net primary production anomalies (Pg C yr^{-1}) using GISS (solid line) and NCEP (dashed line) solar radiation.

[43] The longer temporal extent of the NCEP data, available from 1948 to the present, makes this data set attractive for studies that require these additional years. However, it is recommended that studies of solar radiation effects on ecosystems compare NCEP and GISS data during 1984–2000 to improve confidence of results.

[44] GISS solar radiation declined by 0.4% during 1984–2000, with no obvious upward trend in the 1990s. This behavior is in contrast to the suggestion of an increase in the 1990s discussed by *Cohen et al.* [2004]. Difficulties arise when comparing these two results directly, however. First, *Cohen et al.* [2004] summarized mainly ground-based studies, and second, this study discusses only growing season radiation, not annual radiation. Additional investigation is required to resolve this issue.

[45] Changing solar radiation influenced NPP estimates less than changes in other drivers such as temperature and precipitation, though separation of these factors is difficult because fAPAR responds to all drivers. Most regions experienced changes in solar radiation of 5%. Furthermore, increases in solar radiation often are accompanied by decreases in precipitation (and the reverse) whose influence is typically stronger, thereby masking the influence of solar radiation on NPP. As a result, the indirect effects of solar radiation on NPP through changing fAPAR were not detectable. Regionally, the direct effect caused NPP trend changes of over 10% in some areas during 1984–2000.

[46] Other studies of global carbon fluxes report different results than those found here. *Nemani et al.* [2003] reported an NPP increase in the Amazon River basin of 27%, responsible for driving 40% of their estimated global increase of 6%, and attributed this change to increased solar radiation. In this study, I found lower changes in NPP in this region and little global trend (1% with NCEP solar radiation). Much of this difference was likely due to the different NDVI data sets used (Nemani et al. used the mean of an earlier version of the GIMMS NDVI and the Pathfinder NDVI). Some of the difference was also a result of the different ecosystem models used (CASA versus BIOME-BGC) and the slightly different time periods (1982–1998 versus 1984–2000). *Cao et al.* [2002] used a carbon cycle model driven by observed climate, CO_2 concentrations, and vegetation distribution to compute carbon fluxes in the 1980s and 1990s. In contrast to this study, their estimates were not constrained by satellite observations of fAPAR. The authors estimated that NPP increased by 5% from 1981 to 1998.

[47] The partitioning of incident solar radiation into diffuse versus direct components affects photosynthesis. The addition of clouds and aerosols results in a higher diffuse fraction of total incident radiation that is thought to stimulate photosynthesis through increased radiation on shaded leaves [*Roderick et al.*, 2001]. Higher stratospheric aerosol loadings following the eruption of Mount Pinatubo increased the diffuse fraction [e.g., *Molineaux and Ineichen*, 1996], and *Gu et al.* [2003] reported a resulting increase in photosynthesis in a temperate deciduous forest. In contrast, studies of tree ring records, atmospheric transport models, and ecosystem models find that the cooling effect following an eruption outweighs the effect of additional incident radiation [*Angert et al.*, 2004; *Krakauer and Randerson*, 2003; *Lucht et al.*, 2002]. Changing diffuse versus direction conditions are only considered in CASA through changing vegetation (fAPAR) and are thus a possible source of uncertainty, although it is currently unclear whether these effects have a large impact.

[48] GISS *S* declined in 1991 and 1992. Mount Pinatubo erupted in June 1991, and was responsible for a large part of this decrease [e.g., *Minnis et al.*, 1993; *Molineaux and Ineichen*, 1996]. An El Niño event occurred in 1991–1992, and possible changes in cloudiness in response may have caused reductions in solar radiation. However, GISS *S* was above average during other El Niño events (1986–1987, 1997–1998), suggesting that El Niño effects were minor. In contrast to GISS *S*, NCEP *S* increased in 1991 and 1992, contrary to expected and highlighting the importance of including stratospheric aerosols when studying this time period.

[49] The NPP response in 1991 and 1992 included solar radiation, temperature, and precipitation effects. Both runs show declines from 1990 to 1991, possibly in response to both the Mount Pinatubo eruption and the El Niño, although residual contamination of the processed NDVI by stratospheric aerosols may still exist. The decrease in NPP from 1990 to 1992 was estimated at 2.3 Pg C yr^{-1} as derived from the NCEP solar radiation, but 3.2 Pg C yr^{-1} in the GISS NPP, a 40% increase. The greater difference in GISS NPP resulted from a higher value in 1990 (prior to the eruption) as well as a lower value in 1991. GISS NPP was also substantially lower than NCEP NPP in 1992. Thus the use of GISS solar radiation enhanced the global response of vegetation in the years following the Mount Pinatubo eruption compared to the results using NCEP solar radiation.

5. Conclusions

[50] Global ecosystem models that require solar radiation as input have several alternatives available. Two represen-

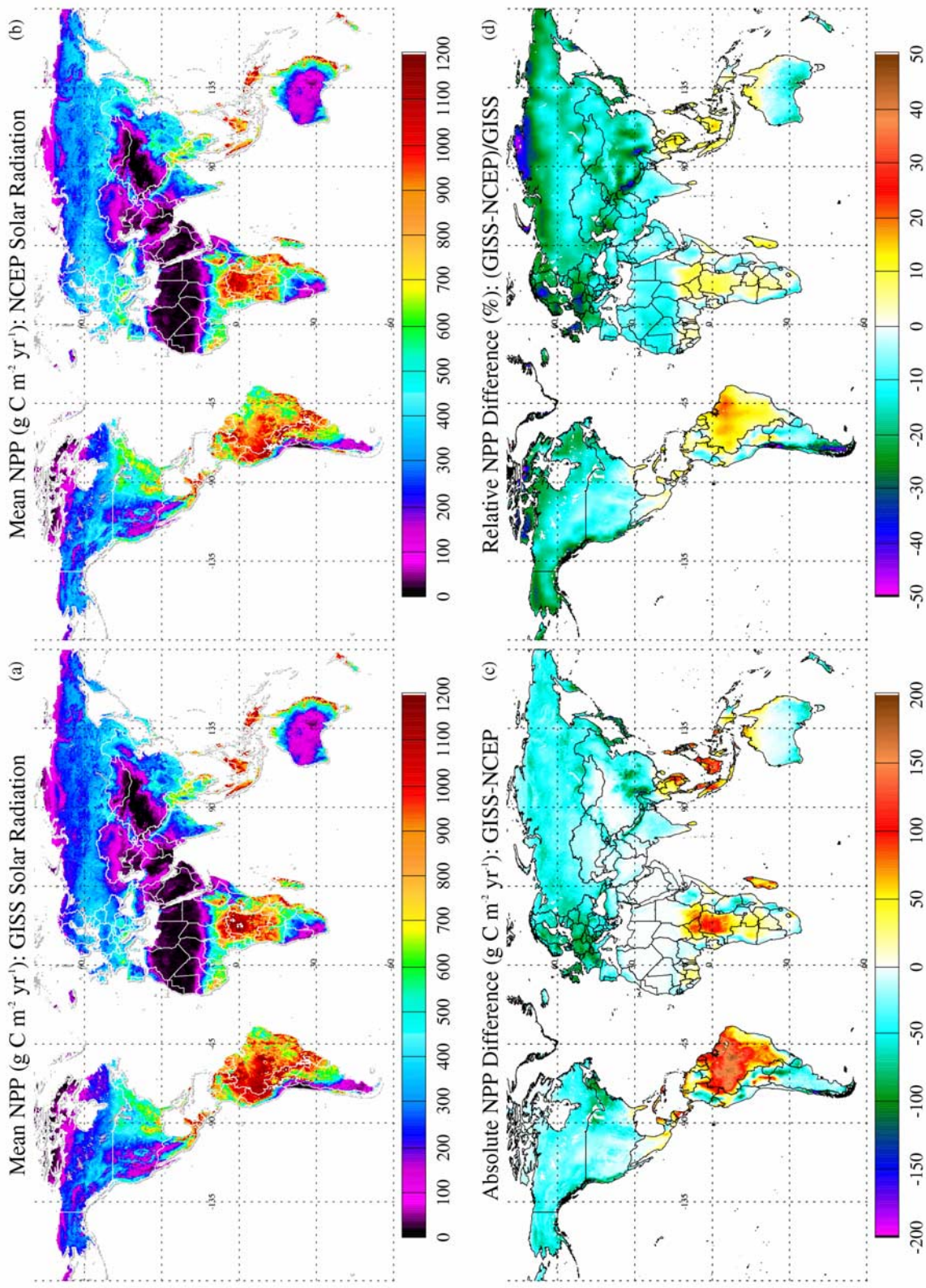

Figure 8. Net primary production averaged over 1984–2000 (g C m^{-2} yr^{-1}) using (a) GISS and (b) NCEP solar radiation. (c) Absolute difference between runs using GISS and NCEP (g C m^{-2} yr^{-1}). (d) Relative difference (%).

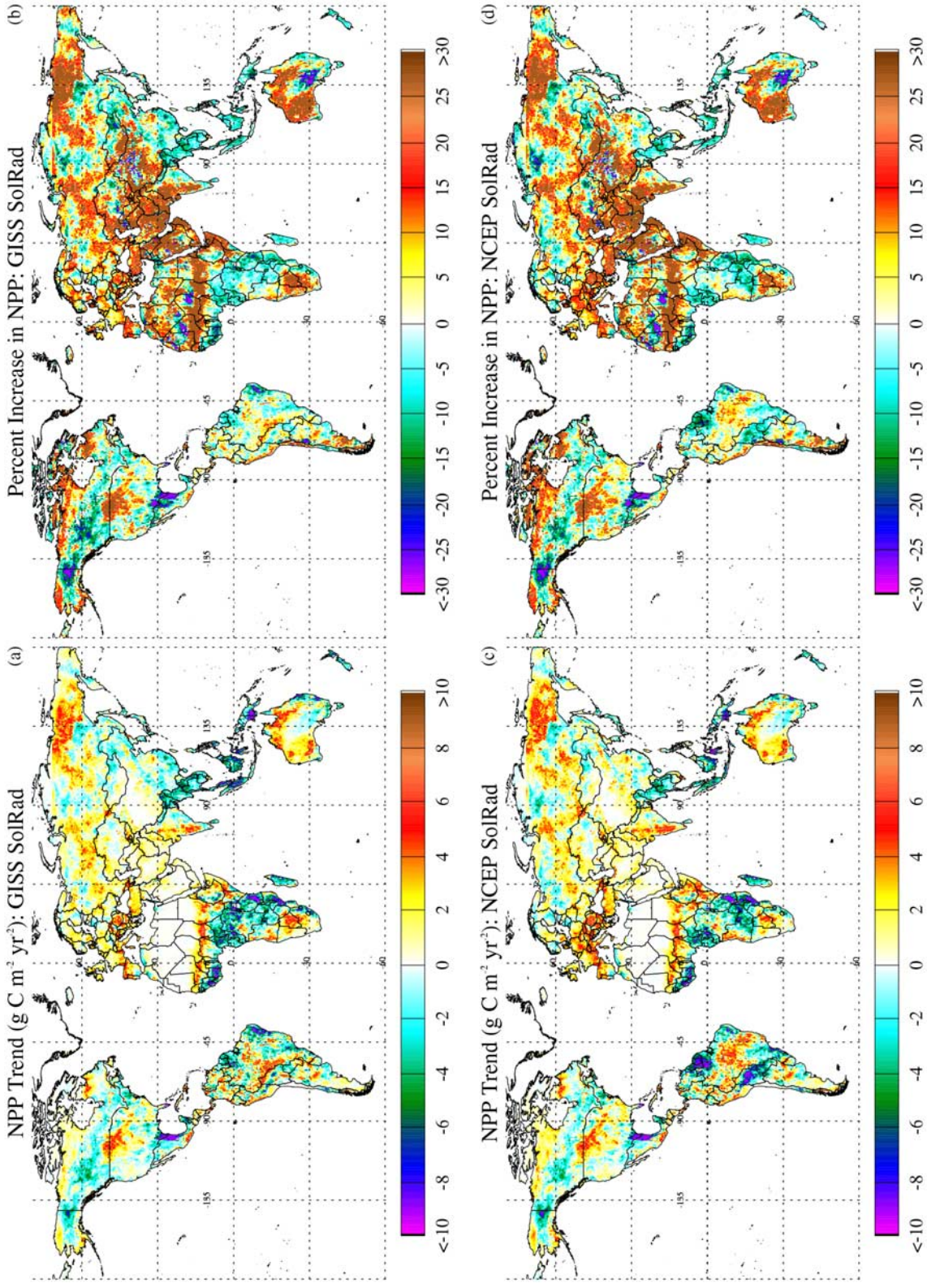

Figure 9. Trend in net primary production from 1984–2000. (a) Absolute trend using GISS data set (g C m^{-2} yr^{-1}). (b) Percent increase using GISS data set. (c) Absolute trend using NCEP data set (g C m^{-2} yr^{-1}). (d) Percent increase using NCEP data set.

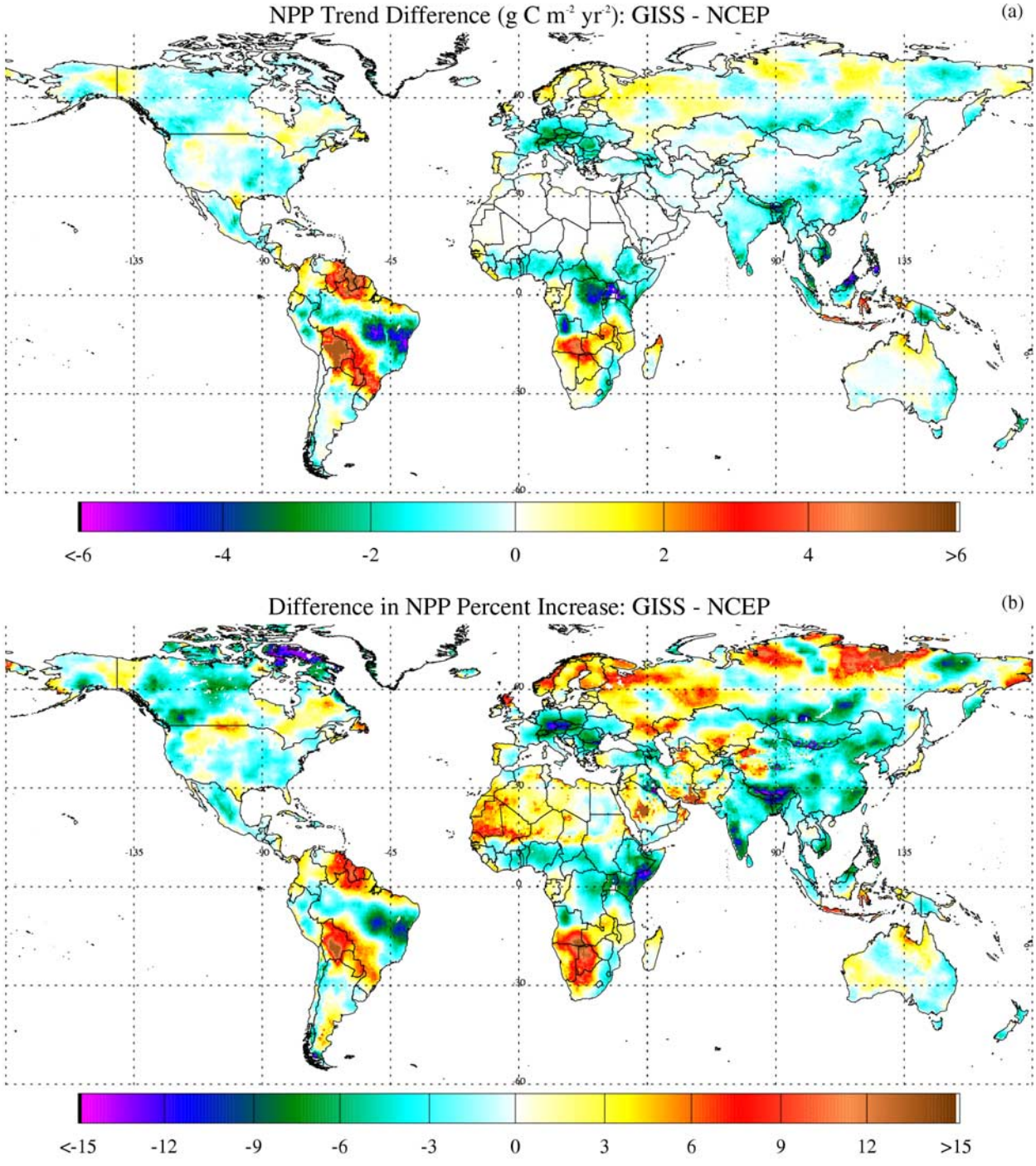

Figure 10. (a) Difference between trends in net primary production from 1984–2000 using GISS and NCEP data sets (g C m^{-2} yr^{-1}). (b) Difference in percent increases; this would be the same as Figure 6b if the same ε^* were used for each run.

tative data sets, one based on satellite-observed clouds (GISS) and one from numerical weather prediction reanalyses (NCEP), were selected for comparison. GISS estimates had substantially reduced errors relative to ground-based observations compared to solar radiation from NCEP. Hence it is recommended that studies utilize GISS solar radiation where possible. However, the temporal extent of the GISS data set (1984–2000) limits the utility of these estimates in longer-term studies. Selection of a solar radiation data set will strongly affect the regional results of models that compute carbon stocks and fluxes (e.g., the net carbon flux) since NPP is the input of carbon into ecosystems.

[51] Globally, GISS growing season solar radiation was lower than the NCEP value by 16% as a result of higher

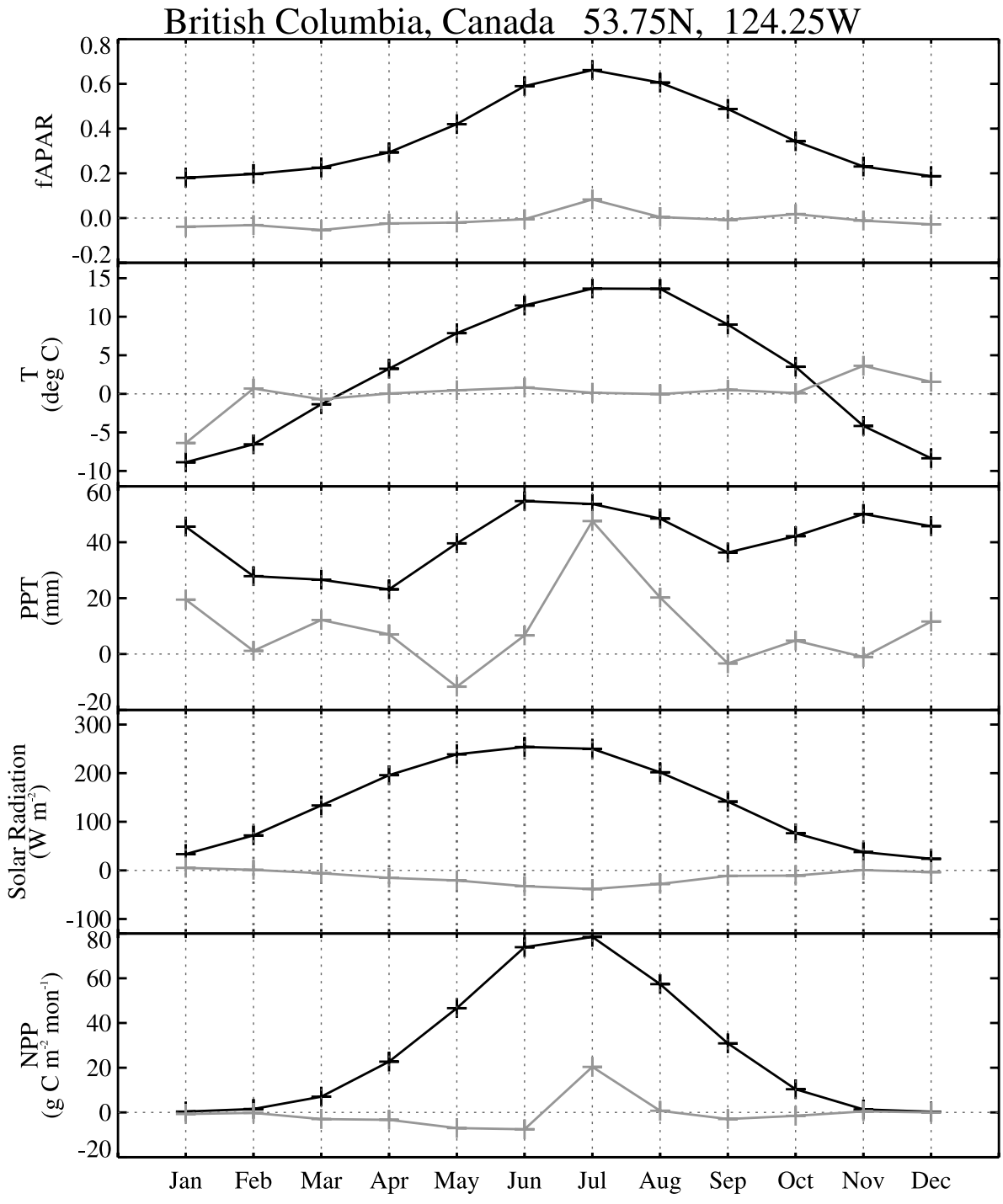

Figure 11. Monthly mean annual cycles and trends from 1984–2000 of inputs and resulting net primary production for the location in British Columbia, Canada, with a large decrease in solar radiation. See Figure 5b for location. Solar radiation is from the GISS data set. Units of trend lines are same as for mean annual cycles (listed at left) but with additional yr^{-1}.

cloudiness. Locally, NCEP values exceeded GISS values by 10–60%. Little trend over the study period (1984–2000) existed in either data set at the global scale, though regional changes in the GISS solar radiation were up to 10%. Differences in percent changes between NCEP and GISS solar radiation were 10% in some areas.

[52] The adjustment of the maximum light use efficiency in the CASA model accounted for the differences in mean solar radiation between the two data sets, leading to similar global NPP means. Local absolute differences in mean NPP were largest in the tropics, and relative differences exceeded 20% in regions throughout the globe. Trends in global NPP

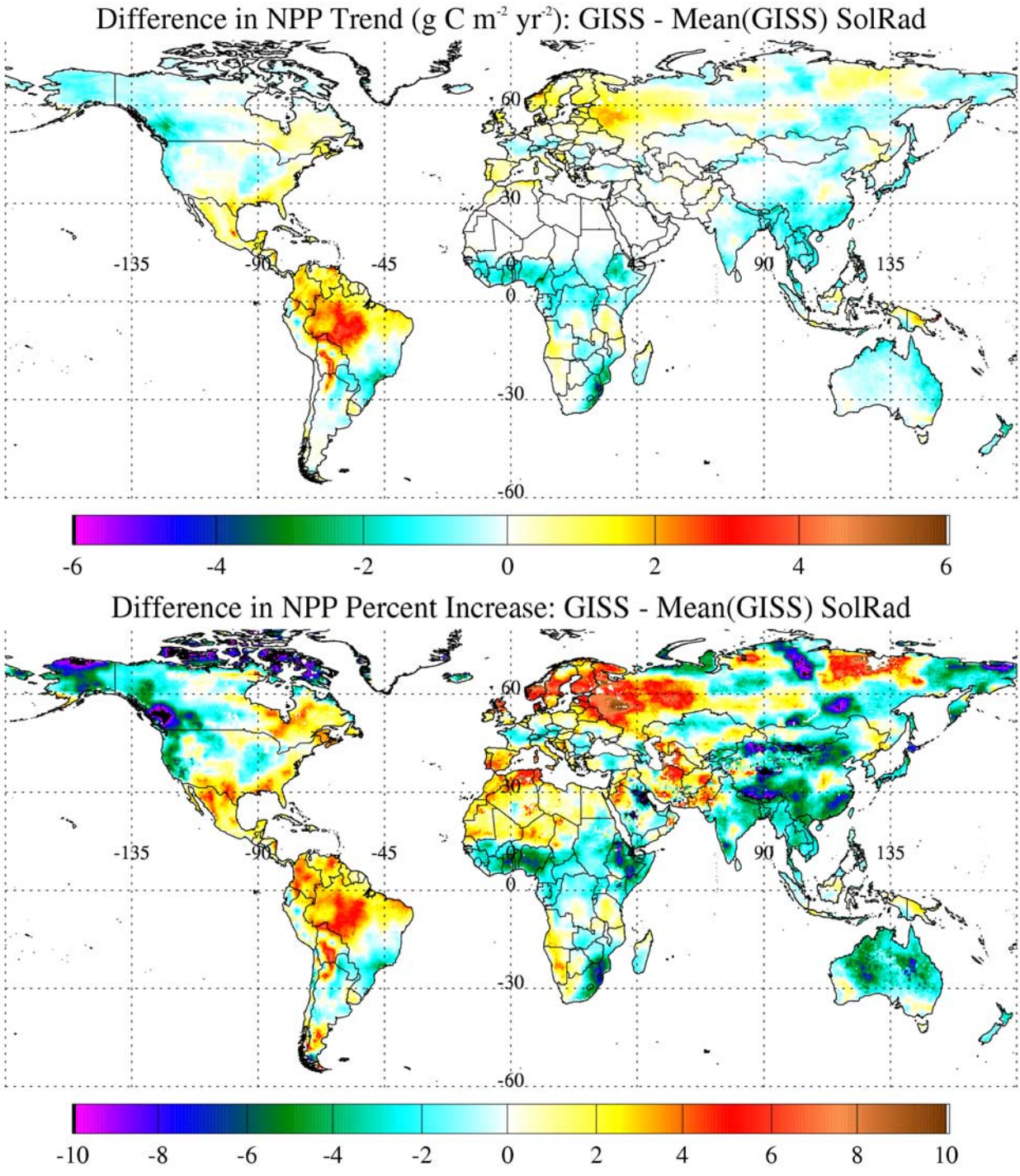

Figure 12. Differences in net primary production trends computed using interannually varying GISS solar radiation and the mean annual cycle of GISS solar radiation. (a) Difference in absolute trends (g C m^{-2} yr^{-1}). (b) Difference in percent increases.

were 1% or less over the study period. Using the GISS solar radiation, local NPP changes of >30% occurred, with differences compared to NPP using NCEP radiation of 10% in some areas.

[53] The indirect effect of solar radiation on production, through changing fAPAR, could not be detected in the satellite observations. This was likely a result of the anti-correlation of solar radiation and precipitation, whose influence is stronger in most ecosystems. The direct effect on NPP trends was assessed by estimating NPP with a mean annual cycle of solar radiation, and resulted in regional differences of up to 10%.

[54] Global NPP increased by 1% using the NCEP solar radiation data set compared to the 6% estimated by *Nemani*

et al. [2003]. The lower value of this study can be attributed to different NDVI data sets, carbon cycle models, and years (1984–2000 in this study, 1982–1999 in the work of *Nemani et al.* [2003]). The NPP increase associated with the GISS solar radiation was smaller throughout much of the globe compared to that using the NCEP reanalysis product. In the Amazon River basin, to which *Nemani et al.* [2003] attributed 40% of their increase, I found substantially larger NPP trends in the northern half of the basin with the GISS data compared to the NCEP data but substantially smaller trends in the southern half of the basin.

[55] The choice of solar radiation data set in ecosystem modeling studies may continue to be driven by availability during the time period of interest. However, for studies during the 1980s and 1990s, GISS solar radiation should be used owing to its inclusion of observed clouds. In addition, studies that investigate the ecosystem consequences of post-Mount Pinatubo atmospheric conditions should include the GISS data that account for changing aerosol conditions. Satellite-derived data sets are better-constrained estimates of solar radiation than those from reanalyses, and should be utilized when possible.

[56] **Acknowledgments.** I am grateful to several groups for supplying data sets: Yuanchong Zhang and Bill Rossow for the GISS solar radiation data set; the NOAA Climate Diagnostic Center, Boulder, Colorado, for the NCEP reanalysis (www.cdc.noaa.gov); Tim Mitchell for the CRU temperatures and precipitation; Hans Gilgen for the GEBA database; and Jorge Pinzon, Molly Brown, and Jim Tucker for the NDVI data set. I would like to thank Chris Field, his research group, and Greg Asner for developing the CASA model, and Dennis Ojima for his support. I would also like to acknowledge the helpful comments of two anonymous reviewers. This work was funded by NSF grant ATM-9979958, NASA grant NAG5-11073, and USGS cooperative agreement 04CRAG0004/4004CS0001.

References

Angert, A., S. Biraud, C. Bonfils, W. Buermann, and I. Fung (2004), CO_2 seasonality indicates origins of post-Pinatubo sink, *Geophys. Res. Lett.*, *31*, L11103, doi:10.1029/2004GL019760.

Bony, S., Y. Sud, K. M. Lau, J. Susskind, and S. Saha (1997), Comparison and satellite assessment of NASA/DAO and NCEP-NCAR reanalyses over tropical ocean: Atmospheric hydrology and radiation, *J. Clim.*, *10*(6), 1441–1462.

Brown, M. E., J. E. Pinzon, and C. J. Tucker (2005), Quantitative comparison of four AVHRR global data sets for land applications, report, 35 pp., NASA Global Mapping and Modell. Syst. (GIMMS), NASA Goddard Space Flight Cent., Greenbelt, Md.

Cao, M. K., S. D. Prince, and H. H. Shugart (2002), Increasing terrestrial carbon uptake from the 1980s to the 1990s with changes in climate and atmospheric CO_2, *Global Biogeochem. Cycles*, *16*(4), 1069, doi:10.1029/2001GB001553.

Cohen, S., B. G. Liepert, and G. Stanhill (2004), Global dimming comes of age, *Eos Trans. AGU*, *85*(38), 362–363.

Cramer, W., D. W. Kicklighter, A. Bondeau, B. S. Moore III, G. Churkina, B. Nemry, A. Ruimy, A. L. Schloss, J. Kaduk, and participants of the Potsdam NPP Model Intercomparison (1999), Comparing global models of terrestrial net primary productivity (NPP): Overview and key results, *Global Change Biol.*, *5*, Suppl., 1–15.

Darnell, W. L., W. F. Staylor, S. K. Gupta, N. A. Ritchey, and A. C. Wilber (1992), Seasonal variation of surface radiation budget derived from International Satellite Cloud Climatology Project C1 data, *J. Geophys. Res.*, *97*(D14), 15,741–15,760.

Field, C. B., J. T. Randerson, and C. M. Malmström (1995), Global net primary production: Combining ecology and remote sensing, *Remote Sens. Environ.*, *51*(1), 74–88.

Food and Agriculture Organization/UNESCO (1971), Soil map of the world, 1:5,000,000, Paris.

Fouquart, Y., B. Bonnel, and V. Ramaswamy (1991), Intercomparing shortwave radiation codes for climate studies, *J. Geophys. Res.*, *96*(D5), 8955–8968.

Gilgen, H., and A. Ohmura (1999), The Global Energy Balance Archive, *Bull. Am. Meteorol. Soc.*, *80*(5), 831–850.

Gilgen, H., M. Wild, and A. Ohmura (1998), Means and trends of shortwave irradiance at the surface estimated from global energy balance archive data, *J. Clim.*, *11*(8), 2042–2061.

Gu, L. H., D. D. Baldocchi, S. C. Wofsy, J. W. Munger, J. J. Michalsky, S. P. Urbanski, and T. A. Boden (2003), Response of a deciduous forest to the Mount Pinatubo eruption: Enhanced photosynthesis, *Science*, *299*(5615), 2035–2038.

Hansen, J., G. Russell, D. Rind, P. Stone, A. Lacis, S. Lebedeff, R. Ruedy, and L. Travis (1983), Efficient 3-dimensional global-models for climate studies: Model-I and Model-II, *Mon. Weather Rev.*, *111*(4), 609–662.

Hansen, J., et al. (2002), Climate forcings in Goddard Institute for Space Studies SI2000 simulations, *J. Geophys. Res.*, *107*(D18), 4347, doi:10.1029/2001JD001143.

Harshvardhan, D. A. Randall, T. G. Corsetti, and D. A. Dazlich (1989), Earth radiation budget and cloudiness simulations with a general-circulation model, *J. Atmos. Sci.*, *46*(13), 1922–1942.

Hicke, J. A., G. P. Asner, J. T. Randerson, C. Tucker, S. Los, R. Birdsey, J. C. Jenkins, and C. Field (2002a), Trends in North American net primary productivity derived from satellite observations, 1982–1998, *Global Biogeochem. Cycles*, *16*(2), 1018, doi:10.1029/2001GB001550.

Hicke, J. A., G. P. Asner, J. T. Randerson, C. Tucker, S. Los, R. Birdsey, J. C. Jenkins, C. Field, and E. Holland (2002b), Satellite-derived increases in net primary productivity across North America, 1982–1998, *Geophys. Res. Lett.*, *29*(10), 1427, doi:10.1029/2001GL013578.

Kalnay, E., et al. (1996), The NCEP/NCAR 40-year reanalysis project, *Bull. Am. Meteorol. Soc.*, *77*(3), 437–471.

Kanamitsu, M. (1989), Description of the NMC global data assimilation and forecast system, *Weather Forecast.*, *4*, 335–342.

Kidwell, K. (1995), *NOAA Polar Orbiter Data Products Users Guide*, 304 pp., Natl. Oceanic and Atmos. Admin., Silver Spring, Md.

Kistler, R., et al. (2001), The NCEP-NCAR 50-year reanalysis: Monthly means CD-ROM and documentation, *Bull. Am. Meteorol. Soc.*, *82*(2), 247–267.

Krakauer, N. Y., and J. T. Randerson (2003), Do volcanic eruptions enhance or diminish net primary production? Evidence from tree rings, *Global Biogeochem. Cycles*, *17*(4), 1118, doi:10.1029/2003GB002076.

Lacis, A. A., and J. E. Hansen (1974), Parameterization for absorption of solar-radiation in Earth's atmosphere, *J. Atmos. Sci.*, *31*(1), 118–133.

Ladd, C., and N. A. Bond (2002), Evaluation of the NCEP/NCAR reanalysis in the NE Pacific and the Bering Sea, *J. Geophys. Res.*, *107*(C10), 3158, doi:10.1029/2001JC001157.

Liepert, B. G. (2002), Observed reductions of surface solar radiation at sites in the United States and worldwide from 1961 to 1990, *Geophys. Res. Lett.*, *29*(10), 1421, doi:10.1029/2002GL014910.

Los, S. O., G. J. Collatz, P. J. Sellers, C. M. Malmstrom, N. H. Pollack, R. S. DeFries, L. Bounoua, M. T. Parris, C. J. Tucker, and D. A. Dazlich (2000), A global 9-yr biophysical land surface dataset from NOAA AVHRR data, *J. Hydrometeorol.*, *1*, 183–199.

Lucht, W., I. C. Prentice, R. B. Myneni, S. Sitch, P. Friedlingstein, W. Cramer, P. Bousquet, W. Buermann, and B. Smith (2002), Climatic control of the high-latitude vegetation greening trend and Pinatubo effect, *Science*, *296*(5573), 1687–1689.

McGuire, A. D., et al. (2001), Carbon balance of the terrestrial biosphere in the twentieth century: Analyses of CO_2, climate and land use effects with four process-based ecosystem models, *Global Biogeochem. Cycles*, *15*(1), 183–206.

McPeters, R. D., et al. (1996), Nimbus-7 Total Ozone Mapping Spectrometer (TOMS) data products user's guide, *NASA Ref. Publ., 1384*, 67 pp.

Minnis, P., E. F. Harrison, L. L. Stowe, G. G. Gibson, F. M. Denn, D. R. Doelling, and W. L. Smith (1993), Radiative climate forcing by the Mount-Pinatubo eruption, *Science*, *259*(5100), 1411–1415.

Molineaux, B., and P. Ineichen (1996), Impact of Pinatubo aerosols on the seasonal trends of global, direct and diffuse irradiance in two northern mid-latitude sites, *Solar Energy*, *58*(1–3), 91–101.

Nemani, R., M. White, P. Thornton, K. Nishida, S. Reddy, J. Jenkins, and S. Running (2002), Recent trends in hydrologic balance have enhanced the terrestrial carbon sink in the United States, *Geophys. Res. Lett.*, *29*(10), 1468, doi:10.1029/2002GL014867.

Nemani, R. R., C. D. Keeling, H. Hashimoto, W. M. Jolly, S. C. Piper, C. J. Tucker, R. B. Myneni, and S. W. Running (2003), Climate-driven increases in global terrestrial net primary production from 1982 to 1999, *Science*, *300*(5625), 1560–1563.

Ohmura, A., and H. Gilgen (1991), The GEBA database: Interactive applications, retrieving data, *Global Energy Balance Archive (GEBA) Rep. 2*, 60 pp., Zucher Geogr. Scrift, Zurich.

Ohmura, A., et al. (1998), Baseline Surface Radiation Network (BSRN/WCRP): New precision radiometry for climate research, *Bull. Am. Meteorol. Soc.*, *79*(10), 2115–2136.

Phillips, T. J. (1996), Documentation of the AMIP models on the World Wide Web, *Bull. Am. Meteorol. Soc.*, *77*(6), 1191–1196.

Pinker, R. T., and I. Laszlo (1992), Modeling surface solar irradiance for satellite applications on a global scale, *J. Appl. Meteorol.*, *31*(2), 194–211.

Potter, C. S., J. T. Randerson, C. B. Field, P. A. Matson, P. M. Vitousek, H. A. Mooney, and S. A. Klooster (1993), Terrestrial ecosystem production: A process model based on global satellite and surface data, *Global Biogeochem. Cycles*, *7I*(4), 811–842.

Potter, C. S., S. Klooster, and V. Brooks (1999), Interannual variability in terrestrial net primary production: Exploration of trends and controls on regional to global scales, *Ecosystems*, *2*, 36–48.

Roderick, M. L., and G. D. Farquhar (2002), The cause of decreased pan evaporation over the past 50 years, *Science*, *298*(5597), 1410–1411.

Roderick, M. L., G. D. Farquhar, S. L. Berry, and I. R. Noble (2001), On the direct effect of clouds and atmospheric particles on the productivity and structure of vegetation, *Oecologia*, *129*(1), 21–30.

Rossow, W. B., and R. A. Schiffer (1999), Advances in understanding clouds from ISCCP, *Bull. Am. Meteorol. Soc.*, *80*(11), 2261–2287.

Rossow, W. B., and Y. C. Zhang (1995), Calculation of surface and top of atmosphere radiative fluxes from physical quantities based on ISCCP data sets: 2. Validation and first results, *J. Geophys. Res.*, *100*(D1), 1167–1197.

Running, S. W., R. R. Nemani, and R. D. Hungerford (1987), Extrapolation of synoptic meteorological data in mountainous terrain and its use for simulating forest evapotranspiration and photosynthesis, *Can. J. For. Res.*, *17*(6), 472–483.

Sasamori, T., J. London, and D. V. Hoyt (1972), Radiation budget of the Southern Hemisphere, *Meteorol. Monogr.*, *35*, 9–22.

Sato, M., J. E. Hansen, M. P. McCormick, and J. B. Pollack (1993), Stratospheric aerosol optical depths, 1850–1990, *J. Geophys. Res.*, *98*(D12), 22,987–22,994.

Schimel, D., et al. (2000), Contribution of increasing CO_2 and climate to carbon storage by ecosystems in the United States, *Science*, *287*(5460), 2004–2006.

Scott, J. D., and M. A. Alexander (1999), Net shortwave fluxes over the ocean, *J. Phys. Oceanogr.*, *29*(12), 3167–3174.

Slingo, J. M. (1987), The development and verification of a cloud prediction scheme for the ECMFM model, *Q. J. R. Meteorol. Soc.*, *113*(477), 899–927.

Stanhill, G., and S. Cohen (2001), Global dimming: A review of the evidence for a widespread and significant reduction in global radiation with discussion of its probable causes and possible agricultural consequences, *Agric. For. Meteorol.*, *107*(4), 255–278.

Tucker, C. J., D. A. Slayback, J. E. Pinzon, S. O. Los, R. B. Myneni, and M. G. Taylor (2001), Higher northern latitude normalized difference vegetation index and growing season trends from 1982 to 1999, *Int. J. Biometeorol.*, *45*(4), 184–190.

VEMAP Members (1995), Vegetation/ecosystem modeling and analysis project: Comparing biogeography and biogeochemistry models in a continental-scale study of terrestrial ecosystem responses to climate change and CO_2 doubling, *Global Biogeochem. Cycles*, *9*(4), 407–438.

Weare, B. C. (1997), Comparison of NCEP-NCAR cloud radiative forcing reanalyses with observations, *J. Clim.*, *10*(9), 2200–2209.

Yang, S. K., Y. T. Hou, A. J. Miller, and K. A. Campana (1999), Evaluation of the earth radiation budget in NCEP-NCAR reanalysis with ERBE, *J. Clim.*, *12*(2), 477–493.

Zhang, Y. C., W. B. Rossow, and A. A. Lacis (1995), Calculation of surface and top of atmosphere radiative fluxes from physical quantities based on ISCCP data sets: 1. Method and sensitivity to input data uncertainties, *J. Geophys. Res.*, *100*(D1), 1149–1165.

Zhang, Y.-C., W. B. Rossow, A. A. Lacis, V. Oinas, and M. I. Mishchenko (2004), Calculation of radiative fluxes from the surface to top of atmosphere based on ISCCP and other global data sets: Refinements of the radiative transfer model and the input data, *J. Geophys. Res.*, *109*, D19105, doi:10.1029/2003JD004457.

J. A. Hicke, Natural Resource Ecology Laboratory, Colorado State University, 1499 Campus Delivery, Fort Collins, CO 80523-1499, USA. (jhicke@nrel.colostate. edu)